ORIGINAL ARTICLE

The role of TLR4/MyD88/NF-κB pathway in periodontitis-induced liver inflammation of rats

Yiyun Yue[1] 🆔 | Xinchan Liu[2] | Yan Li[1] | Boyuan Xia[1] | Weixian Yu[2,3] 🆔

[1]Department of Periodontology, Jilin University, Changchun, China

[2]Department of Geriatric Stomatology, Jilin University, Changchun, China

[3]Jilin Provincial Laboratory of Biomedical Engineering, School and Hospital of Stomatology, Jilin University, Changchun, China

Correspondence
Weixian Yu, Department of Periodontology, Department of Geriatric Stomatology, Jilin Provincial Laboratory of Biomedical Engineering, School and Hospital of Stomatology, Jilin University, Changchun 130021, China.
Email: yu-wei-xian@163.com

Abstract

Objectives: The aim of this study was to clarify the immune mechanism of hepatic injury induced by periodontitis using a rat model.

Methods: Twenty-four SPF male Wistar rats were randomly divided into two groups: control group (CG) and periodontitis group (PG). In order to induce experimental periodontitis, we tied the wire ligature around bilateral maxillary first molar of rats. After 8 weeks, the following indicators were valued: gingival index, tooth mobility, probing pocket depth; indexes about oxidative stress and circulating biomarkers; bone retraction by micro-CT analysis; Toll-like receptor 4 (TLR4), myeloid differential protein-88 (MyD88), and nuclear factor kappa B (NF-κB) by qRT-PCR and Western blotting; tumor necrosis factor α (TNF-α), and interleukin-6 (IL-6) by qRT-PCR and immunohistochemical staining; inflammation of periodontal and hepatic tissues by histopathological observation.

Results: Periodontal indicators and micro-CT results showed the raised levels of inflammatory response and bone retraction in PG compared with CG. The mRNA and protein levels of TLR4, MyD88, NF-κB, TNF-α, and IL-6 have indicated high values in PG versus CG. Histopathological analysis revealed a correlation between periodontitis and hepatic injury.

Conclusion: TLR4/MyD88/NF-κB pathway may play a role in periodontitis-induced liver inflammation of rats.

KEYWORDS
hepatic inflammation, immune, oxidative stress, periodontitis

1 | INTRODUCTION

Periodontitis is an inflammatory oral disease characterized by periodontal pathogenic bacteria as the initiating factor and the destruction of periodontal supporting tissues, that are gingiva, periodontal membrane, and alveolar bone resorption (Kinane, Stathopoulou, & Papapanou, 2017), affecting most of the adults worldwide (Bellentani, 2017; Eke et al., 2015). One of the pathogenic factors of periodontitis is imbalance in the host reactions caused by the appearance and persistence of dysbiotic oral microbiota and other metabolites that cause the overproduction of inflammatory mediators. In addition, periodontitis can induce an imbalance between oxidant and antioxidant agents, ultimately causes the periodontal tissue damages (Hajishengallis, 2015).

Multiple studies have demonstrated that periodontitis can harm patients' overall health by increasing the risk of diabetes, atherosclerosis, rheumatoid arthritis, Alzheimer's disease, adverse pregnancy outcomes, and hepatic diseases (Hegde & Awan, 2019; Liccardo et al., 2019; Potempa, Mydel, & Koziel, 2017; Wang, Ho, Leung, Goto, & Chang, 2019). The possible causes of the link between periodontitis and systemic diseases represent the spread of periodontal inflammatory mediators, pathogen-induced virulent factors, and oral bacteria through blood circulation and gut microbiota (Hajishengallis, 2015; Konkel, O'Boyle, & Krishnan, 2019; Lamont, Koo, & Hajishengallis, 2018).

Non-alcoholic fatty liver disease (NAFLD), which generally manifest non-alcoholic fatty liver (NAFL), can develop to non-alcoholic steatohepatitis (NASH), liver fibrosis, cirrhosis, and hepatocellular carcinoma (HCC) (Van De Wier, Koek, Bast, & Haenen, 2017) and is characterized by steatosis (fat accumulation) in more than five percent of the hepatocytes in individuals other than alcohol, viruses, drugs, and other specific liver damage factors such as autoimmunity (Sanyal et al., 2011). NAFLD is one of the most common chronic liver diseases and currently estimated to affect a quarter of the general population worldwide (Younossi et al., 2018).

Many studies have reported that oxidative stress and gut microbiota are the important factors related to the pathophysiological mechanism of steatosis and inflammation occurred in NAFLD (Borrelli et al., 2018; Jayakumar & Loomba, 2019; Tripathi et al., 2018). The overproduction of ROS can cause a breakdown of lipid homeostasis which leads to excessive lipid accumulation in hepatocyte. Oxidative stress and lipid peroxidation can induce the release of pro-inflammatory cytokines, such as TNF-α and IL-6, which ultimately promote the evolution of hepatic injury (Kim et al., 2019). In addition, accumulating evidence also implicates the gut microbiota as an emerging cause of NAFLD (Jayakumar & Loomba, 2019). It is reported that some oral bacteria which are associated with periodontitis, including *Porphyromonas gingivalis* (*P. gingivalis*) (Yoneda et al., 2012) and *Aggregatibacter actinomycetemcomitans* (*Aa*) (Komazaki et al., 2017), may be associated with the development and progression of NAFLD. Furthermore, the LPS is the main virulence factor of these bacteria. Miyako et al (Fujita et al., 2018) have demonstrated that *P. gingivalis*-LPS injected into the gingiva can reach to liver in rats. TLR4, mostly expressed on kupffer cells (KCs), which are the liver-derived macrophages, is the main ligand for LPS (Brun, Castagliuolo, Pinzani, Palu, & Martines, 2005; Paik et al., 2003). It can be activated by LPS and lead to the increased hepatic expression of MyD88 and NF-κB, and rise in TNF-α and IL-6 expression (Moretti & Blander, 2014).

Our previous study has found that the expressions of pro-inflammatory cytokines in liver tissues of mice with periodontitis were significantly increased, but the mechanism is still unclear. Thus, we used a Wistar rat model of periodontitis to clarify this point.

2 | MATERIALS AND METHODS

2.1 | Animals

All Wistar rats were purchased from the Experimental Animal Laboratory of Jilin University. Twenty-four male Wistar rats, 8 weeks old, weighing 200-220 g, were housed in a room under controlled temperature at 22 to 25℃, with 12-hr light–dark cycle and a humidity of 55 to 70%. All rats were kept for one week for adjustable feeding before the experiment and had free access to food and water. This study was approved by the Animal Ethics Committee of Jilin University Medical Centre (Jilin, China). The study was performed in accordance with the guidelines laid down by the National Institute of Health (NIH) in the United States regarding the care and use of animals for experimental procedures.

2.2 | Experimental design

In this study, all rats were randomly divided into two groups, 12 rats per group, as follows: control group (CG, without ligature) and periodontitis group (PG, with ligature). The experimental periodontitis was established under intraperitoneal anesthesia of 2% pentobarbital sodium (0.2ml/100g). A wire ligature was placed around the upper 1st molar of each animal bilaterally. The ligatures were checked daily after the application. If the ligature disappears, the new ligature will be placed. After 8 weeks, all rats were euthanized. The liver and body weights were collected in order to calculate liver index (Vasconcelos et al., 2019). Blood serum was collected into tubes by abdominal aortic method, stored at room temperature for 1h, then centrifuged at 4°C, 3,000 rpm, 10 min, isolated, and frozen at −80°C. Then, the upper jaw bone and liver were collected for following tests.

2.3 | Periodontal disease parameters

To assess the severity of periodontal disease, we measured upper 1st molar of each animal. Gingival index (GI) was scored on the basis of: 0 = normal gingival; 1 = mild inflammation, minor change in color, slight edema, and without bleeding on probing; 2 = moderate inflammation, glazing, edema, redness, and bleeding on probing; and 3 = sever inflammation, extreme redness and edema, presence of ulceration, and tendency to spontaneous bleeding (Xu & Wei, 2006).

Tooth mobility (TM) was elevated according to the following scale: 0 = physiological mobility; 1 = slight mobility in buccolingual direction; 2 = moderate mobility in buccolingual and mesiodistal directions; and 3 = severe mobility in buccolingual, mesiodistal, and vertical directions (Mester et al., 2019).

Values of probing pocket depth (PPD) were measured using a round-ended probe with a tip of 0.3mm in diameter. Three sites, mesiobuccal, distobuccal, and midbuccal, were scored, and the average was calculated.

2.4 | Micro-CT analysis of alveolar bone

We used micro-CT system (Scanco, µCT50, Switzerland) to scan the samples. The X-ray tube of the system was set on 70 kV, 200 mA, and 300 msec exposure time. The data sets were reconstructed into three-dimensional volumes with an isotropic nominal resolution of 2048 × 2048 pixels and a voxel size of $10 \times 10 \times 10 \ \mu m^3$. Image processing was performed using the µCT Evaluation Software Program (Scanco, µCT50, Switzerland). To determinate the bone volume changes, the 3-dimensional region of interest (ROI) was defined as a circular cylinder that vertically as the distance from the root bifurcation of the upper 1st molar to the depth of 5 mm. The microstructural parameters of bone, including bone mineral density (BMD) and bone volume/tissue volume (BV/TV), were evaluated.

2.5 | Assessment of laboratory assays, oxidative stress parameters

To evaluate hepatic injury and oxidative stress markers, ALT, AST, gamma-glutamyl transpeptidase (GGT), alkaline phosphatase (AlkP), TC, TG, total antioxigenic capacity (T-AOC), SOD, and malondialdehyde (MDA) were measured according to the manufacturer's indications (Jiancheng Bioengineering Institute, Nanjing, Jiangsu, China).

2.6 | Histological evaluation of periodontal and liver tissues

2.6.1 | H&E staining

Specimens were collected from the periodontal and liver (left lobe) tissues. The following processes were according to Mester et al (Mester et al., 2019) with slight modifications. After fixing in 10% phosphate-buffered formalin (pH 7.2) for 24 hr, maxillary bones were further decalcified by 15% ethylene diamine tetraacetic acid (EDTA). Then, all samples were dehydration, embedded in paraffin, cut into 5-µm sections, heated in the slide warmer for 2 hr, and then stained with hematoxylin and eosin (H&E).

2.6.2 | Immunohistochemistry staining

Immunohistochemistry was used to measure the expressions of TLR4, MyD88, TNF-α, and IL-6 in liver tissues of rats. After routine histological preparation, the sections were deparaffinized with xylene and graded ethanol and washed using deionized water. Then, heating the slides in 0.01 M sodium citrate buffer (pH 6.0) using a microwave and maintain at a subboiling temperature for eight minutes, cool naturally to room temperature. Endogenous peroxidase was blocked with 3% H_2O_2 for twenty minutes. Following, blocking non-specific reactivity with 5% bovine serum albumin (BSA). Afterward, these sections were incubated with primary antibodies: TLR4, MyD88, and IL-6 (1:100, ProteinTech, USA), TNF-α (1:100, Novus, USA), overnight at 4℃. After washing with phosphate-buffered saline (PBS), the sections were incubated with secondary antibody (ZSGB-BIO, PV-9001) for 40 min at 37℃. Finally, 3,3-diaminobenzidine DAB (ZSGB-BIO, ZLI-9018) was used for color staining and hematoxylin was used for counterstaining. The photomicrographs were captured using the light microscopy (Olympus, BX 51, Japan).

2.6.3 | Oil Red O staining

To evaluate hepatic steatosis, 10-µm frozen sections of the liver were stained with Oil Red O kit (Solarbio Science & Technology Ltd., Beijing, China).

2.6.4 | Immunofluorescence method

Immunofluorescence was used to measure the expression of NF-κB p65. The frozen sections of the liver were fixed by 4% paraformaldehyde (PFA), then processed by rupturing membranes with 0.3% Triton X-100 for 30 min, and then blocked with 5% BSA for 1h, and all above were operated at room temperature (RT). Sections were subsequently incubated with primary antibody NF-κB p65 (1:100, Cell Signaling Technology, USA) at 4℃ overnight. After that, sections were incubated with secondary antibody Alexa Fluor 488-conjugated goat anti-rabbit IgG (H + L) (1:100, ProteinTech, USA) for 2h at RT in the dark. Finally, nuclei were stained with DAPI (Solarbio Science & Technology Ltd., Beijing, China). All images were captured using a laser scanning confocal microscope (LSCM) (Olympus, FV3000, Japan).

2.7 | qRT-PCR analysis

Liver tissues were collected and rapidly frozen in liquid nitrogen and then stored at −80℃. The total RNA was extracted from liver tissues with TRIzol reagent (Invitrogen). cDNA was prepared from 1,000 ng total RNA using the PrimeScript RT Reagent Kit (TaKaRa, Japan). Afterward, qRT-PCR was performed using the SYBR PrimeScript qRT-PCR analysis system (TaKaRa, Japan). The conditions for qRT-PCR were as follows: 30 s at 95℃, 40 cycles at 95℃ for 5 s, and 60℃ for 20 s. For data normalization, the housekeeping gene *β-actin* was used as the internal control. To provide analytical replicates, all experiments were repeated three times. Data were analyzed using the $2^{-\Delta\Delta Ct}$ method.

The primer for rat genes is as follows:

TLR4: 5′- CTCACAACTTCAGTGGCTGGATTTA-3′ and
5′-GTCTCCACAGCCACCAGATTCTC-3′

MyD88: 5′- TATACCAACCCTTGCACCAAGTC −3′ and
5′-TCAGGCTCCAAGTCAGCTCATC-3′

NF-κB: 5′-CGACGTATTGCTGTGCCTTC-3′ and
5′-TTGAGATCTGCCCAGGTGGTA-3′

TNF-α: 5′-GGCGTGTTCATCCGTTCTC-3′ and
5′-CTTCAGCGTCTCGTGTGTTTCT-3′
IL-6:5′-ATTGTATGAACAGCGATGATGCAC-3′ and
5′-CCAGGTAGAAACGGAACTCCAGA-3′
β-actin: 5′-GAGAGGGAAATCGTGCGTGACA-3′ and
5′-CGATAGTGACCTGACCGTCA-3′

2.8 | Western blot analysis

Liver tissues were collected and homogenized in RIPA Lysis Buffer (Cell Signaling Technology, USA) containing PMSF and centrifuged at 12,000*g* at 4°C for 15 min. The concentration of protein samples was measured by BCA Protein Assay (Cell Signaling Technology, USA). A total of 35 μg protein for each sample were loaded, diluted with 5 × SDS-PAGE Sample Loading Buffer (Beyotime, Shanghai, China), and heated at 95°C for 5 min. Then, the proteins underwent electrophoresis by 10% SDS-PAGE and transferred to a polyvinylidene difluoride (PVDF) membrane. Then, the membranes were incubated in blocking buffer for 1.5 hr. Afterward, the membranes were incubated with the primary antibodies of TLR4 (1:1,000, ProteinTech, USA), MyD88, NF-κB p65, IκBα, and p-IκBα (1:1,000, Cell Signaling Technology, USA), β-actin (1:10,000, ProteinTech, USA), overnight at 4°C, washed with TBST (tris buffered saline with Tween), and incubated with secondary antibody (1:8,000, ProteinTech, USA) for 2 hr at room temperature. After

five 10-min washes, the expressions of proteins were analyzed by ECL (ProteinTech, USA) detection. The gray value of each band was measured using Image J software.

2.9 | Statistical analysis

All data, expressed as mean ± standard error of the mean (*SEM*), were statistically analyzed using Graphpad Prism 6.0. Comparisons between two groups were analyzed with unpaired *t* test. Values of $p < .05$, $p < .01$ were considered to be statistically significant.

3 | RESULTS

3.1 | Periodontal disease parameters

There were no changes in the CG. The periodontal tissue of PG revealed inflammatory activity, presented redness, severe edema, and bleeding of gingiva (Figure 1a and 1b). GI, PPD, and mobility of upper 1st molar were significantly higher in PG than CG (Table 1). Reconstructed 3D micro-CT images of upper alveolar bone viewed from the buccal direction (Figure 1c and 1d). Micro-CT parameters indicated that the rats of PG had severe alveolar bone resorption, lower bone mineral density (BMD), and bone volume/tissue volume (BV/TV) values versus the CG ($p < .05$) (Table 1).

FIGURE 1 Clinical and pathological findings of periodontal tissue. (a, c, e) Control group. Normal clinical and morphological findings ; (b, d, f) periodontitis group. (b) The arrow represents the 1st molar. Clinical aspect of the periodontitis group, presenting gingival swelling with color alteration, severe edema, and bleeding after slight probe. (d) Severe bone retraction on buccal (the arrow). (f) Sever inflammatory infiltrates of periodontal tissue (the arrow) and bone matrix resorption (the asterisk), bar = 1 mm [Colour figure can be viewed at wileyonlinelibrary.com]
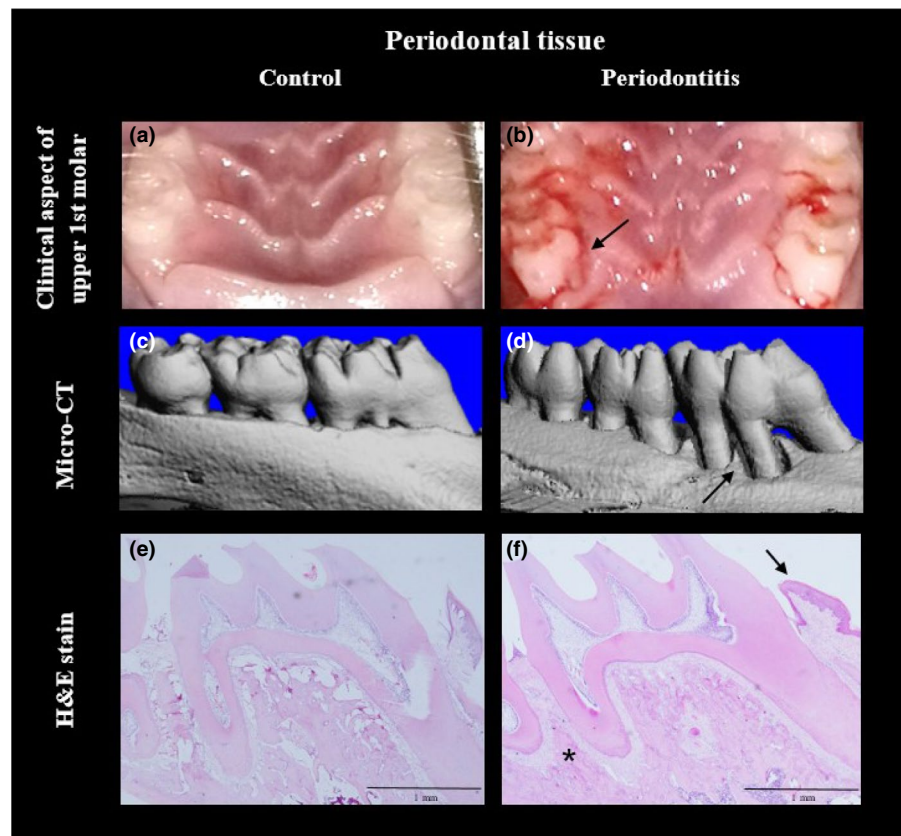
TABLE 1 Periodontal disease, blood, and liver biomarkers

	Control	periodontitis
Periodontal parameters		
GI	0.00 ± 0.00	2.25 ± 0.13***
PPD (mm)	0.21 ± 0.01	2.79 ± 0.09***
TM	0.00 ± 0.00	2.00 ± 0.17***
BMD (mg/cm^3)	747.00 ± 4.92	618.60 ± 8.84**
BV/TV (%)	84.21 ± 0.89	72.87 ± 0.23**
Weight parameters		
Body (g)	332.10 ± 3.45	272.30 ± 10.69***
Liver		
Relative (%)	2.63 ± 0.04	3.50 ± 0.17***
Absolute (g)	8.73 ± 0.10	9.38 ± 0.28*
Blood biomarkers		
AST (U/L)	39.03 ± 2.84	$51.82 \pm$ *
ALT (U/L)	36.05 ± 1.41	47.85 ± 3.24*
AlkP (U/L)	45.74 ± 3.59	70.06 ± 5.85**
GGT (U/L)	3.95 ± 0.44	6.14 ± 0.79*
Total cholesterol (mmol/L)	1.68 ± 0.10	2.33 ± 0.12***
Triglycerides (mmol/L)	0.43 ± 0.02	0.66 ± 0.08**
T-AOC (mM)	0.48 ± 0.01	0.37 ± 0.01*
SOD (U/ml)	102.10 ± 2.26	107.90 ± 2.47
MDA (nmol/ml)	10.65 ± 0.23	23.34 ± 2.02**
Liver biomarkers		
Total cholesterol (μmol/gprot)	22.30 ± 1.29	37.06 ± 3.06*
Triglycerides (μmol/gprot)	41.24 ± 2.55	72.55 ± 2.90*
MDA (mol/gprot)	14.62 ± 1.48	45.82 ± 7.44*

*$p < .05$.
**$p < .01$.
***$p < .001$.

3.2 | Body and liver weights; serum and liver parameters

The value of body and liver weights presented difference ($p < .05$) between the CG and PG (Table 1). The liver index of the PG was higher than the CG ($p < .01$).

Serum levels of AST, ALT, AlkP, and GGT presented higher in the PG versus the CG ($p < .05$) (Table 1). In addition, hepatic and serum levels of TC, TG, and MDA were shown to be increased in the PG compared to the CG, while the level of T-AOC showed the opposite ($p < .05$). SOD presented higher levels in the PG than in the CG, but with no statistical differences ($p > .05$) (Table 1).

3.3 | Histological evaluation of the periodontal and the liver tissues

3.3.1 | Periodontal tissue

There were no significant changes of the periodontium in the CG (Figure 1a, c, and e). In PG, the periodontal tissue has inflammatory activity (Figure 1b). It was characterized by the infiltrations of numerous defense cells in the gingiva and periodontal ligament,

hyperplasia of rete ridges, and destruction of the structural integrity of the junctional epithelium (Figure 1f). Furthermore, the alveolar bone resorption was more severe than the CG (Figure 1d and f).

3.3.2 | Liver tissue

Visualization of the gross morphology of livers from the PG revealed that they were enlarged and had a pale color than the CG (Figure 2a and b). No obvious histological changes observed in the liver tissues of the CG (Figure 2c and e). However, inflammation and steatosis were presented in PG (Figure 2d and f).

The immunohistochemistry results indicated that the expressions of TLR4, MyD88, TNF-α, and IL-6 of liver tissues in PG were more obvious versus the CG (Figure 3).

The immunofluorescence results showed the expression of NF-κB in PG was more obvious than the CG (Figure 4).

3.4 | qRT-PCR

We next determined the mRNA levels of *TLR4*, *MyD88*, *NF-κB*, *TNF-α*, and *IL-6* in the liver tissues. The qRT-PCR analysis presented a

FIGURE 2 Clinical and pathological findings of liver tissue. (a, c, e) Control group. Normal clinical and morphological findings ; (b, d, f) periodontitis group. (b) Gross examination of the liver shows slight enlargement and paler color. (d) Inflammation and steatosis, bar = 100 μm. (f) The arrow represents the lipid droplet (red positive area), bar = 100 μm [Colour figure can be viewed at wileyonlinelibrary.com]
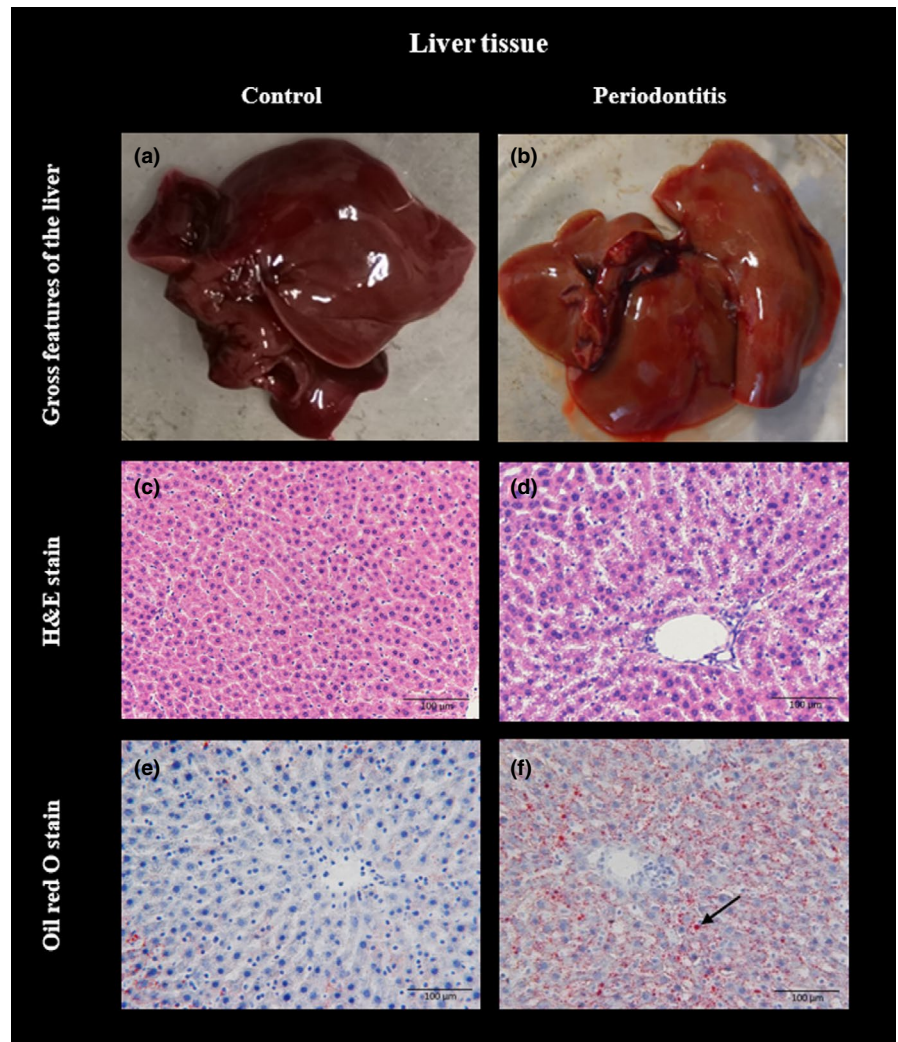
significant upregulation in the expression of *TLR4*, *MyD88*, *NF-κB*, *TNF-α*, and *IL-6*, in the PG compared to the CG (Figure 5).

3.5 | Western blotting

The Western blot results of liver tissues clearly showed that the levels of TLR4, MyD88, NF-κB p65, and p-IκBα were significantly higher in the PG than the CG, while the result of IκBα was the opposite (Figure 6).

4 | DISCUSSION

The relationship between periodontitis and NAFLD has attracted wide public concern recently (Akinkugbe et al., 2017; Sasaki et al., 2018; Tomofuji et al., 2007, 2009). Yoneda et al (Yoneda et al., 2012) have found that the prevalence of *P. gingivalis* infection was significantly higher in the NAFLD patients compared to the healthy subjects, and periodontal treatments may improve the condition of NAFLD of which have periodontitis. In addition,

acceleration of NAFLD in high-fat diet mice infected with *P. gingivalis* was also obvious. Several studies have demonstrated that ligature-induced periodontitis can cause hepatic inflammation and steatosis in rats (Pessoa et al., 2018; Tomofuji et al., 2007, 2009; Vasconcelos et al., 2017). However, the mechanism of that is still unclear. Our study aims to report its correlation view on specific inflammatory mechanism using Wistar rat model with ligature-induced periodontitis for a longer period than other studies (Dos Santos et al., 2017; Pessoa et al., 2018; Vasconcelos et al., 2017).

As a result of the similarities which are in anatomical and histological aspects with the human beings, the rat model can be used in the establishment of periodontal disease, which simulates several characteristics of human periodontitis, such as inflammatory cell infiltration, loss of attachment, and alveolar bone loss (Di Paola et al., 2004; Mester et al., 2019; Srivastava, Neupane, Kumar, & Kohli, 2016; Xue et al., 2018; Yu et al., 2017, 2019). To quantify the severity of periodontitis, the periodontal parameters indicated significant changes between the PG and the CG, which sustained by the micro-CT and histological results. The assessments above proved the effectiveness of experimental construction of periodontitis.
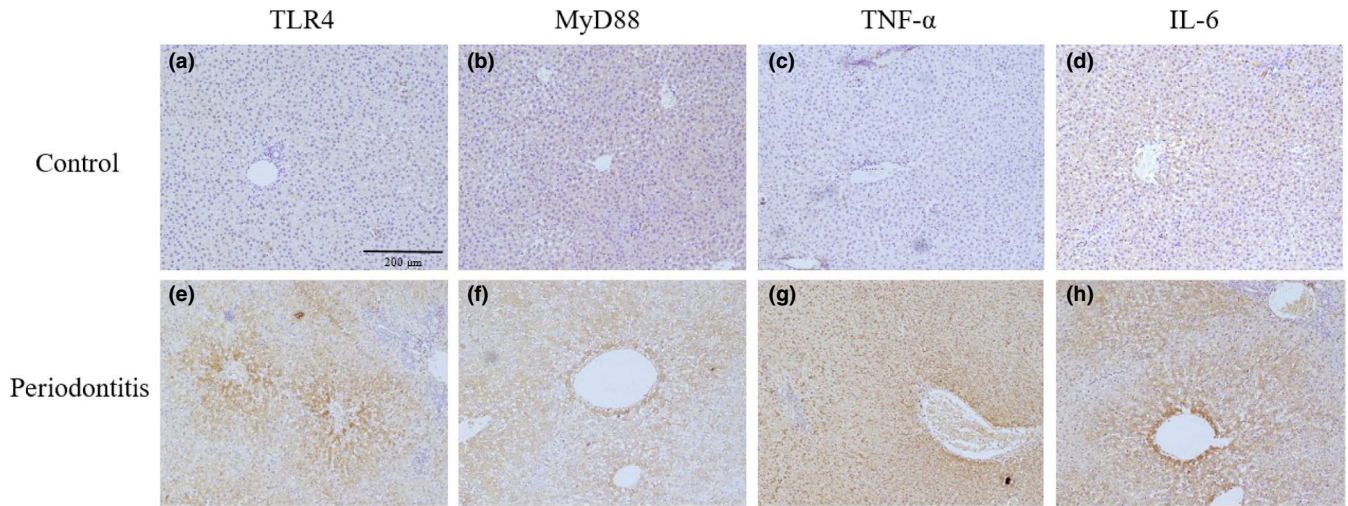
FIGURE 3 Expressions of TLR4, MyD88, TNF-α, and IL-6 in rat liver tissues, assessed by immunohistochemistry technology. The protein expression levels of (a,e) TLR4, (b,f) MyD88, (c,g) TNF-α, and (d,h) IL-6 were significantly higher in periodontitis group than the control group (bar = 200 μm) [Colour figure can be viewed at wileyonlinelibrary.com]
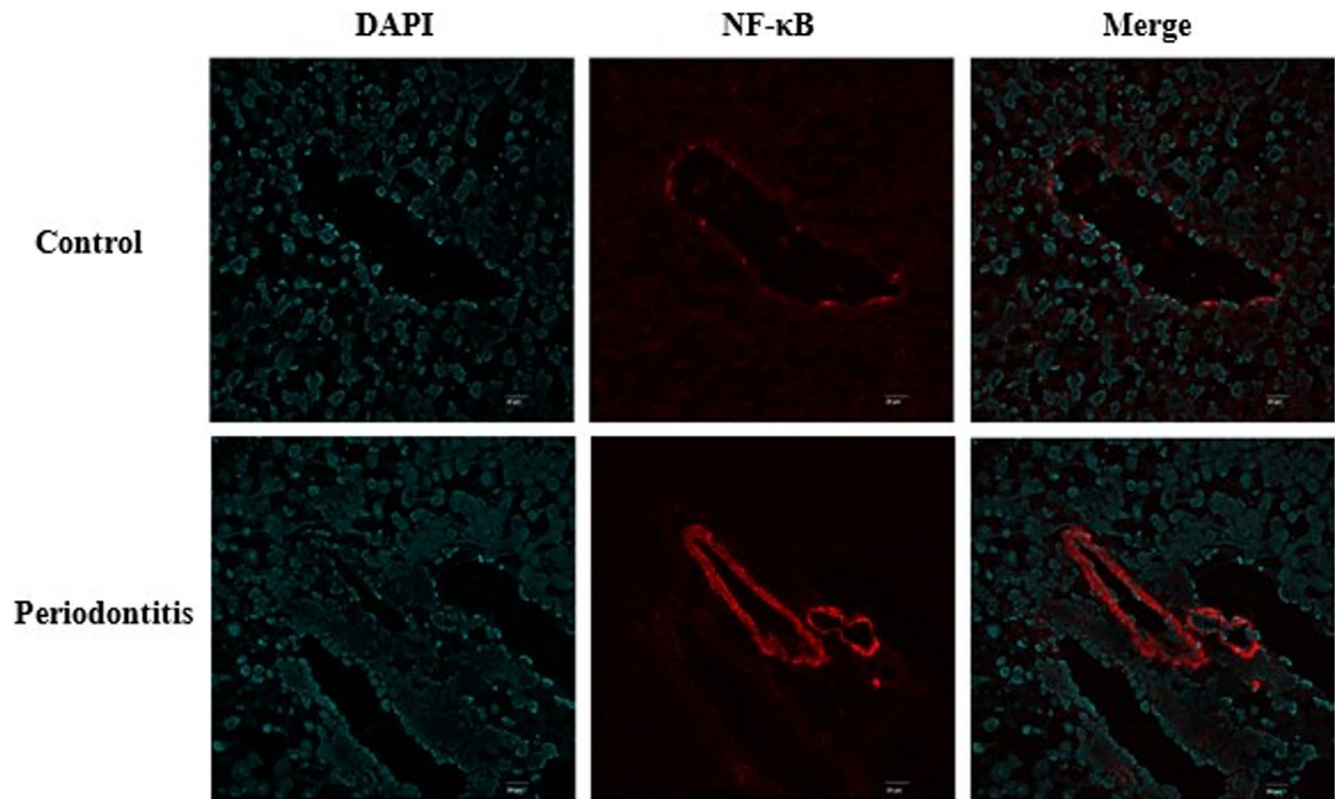

FIGURE 4 Expression of NF-κB protein in rat liver tissue by immunofluorescence staining observed via laser scanning confocal microscopy (LSCM) (magnification, bar = 20μm). Positive NF-κB cells were stained red, and the sections were counterstained with DAPI to visualize the nuclei [Colour figure can be viewed at wileyonlinelibrary.com]

The levels of serum and liver parameters of TC and TG were significantly increased in the PG compared to the CG (Table 1). The histological results also showed the lipid accumulation of liver tissues in periodontitis subjects (Figure 2), which are in accordance with previous studies (Dos Santos et al., 2017; Vasconcelos et al., 2017, 2019), again confirmed by our team. In addition, the levels of AST, ALT, and AlkP were also changed (Table 1).

Periodontal inflammatory mediators and pathogen-induced virulent factors that produced from periodontal structures can be released into blood circulation. In addition, oral bacteria can be translocated to systemic circulation via bloodstream or gut microbiota (Hajishengallis, 2015; Konkel et al., 2019; Lamont et al., 2018). These processes can cause an imbalance between oxidant and antioxidant agents that induce overproduction of lipid peroxidation
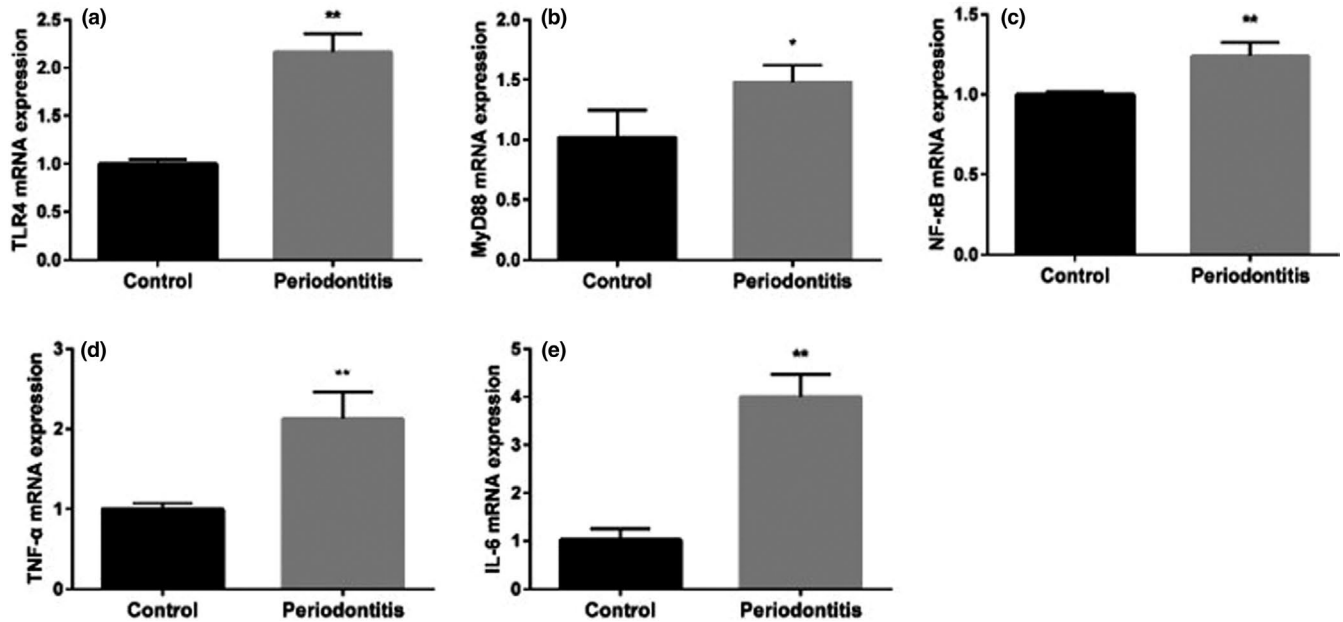
FIGURE 5 Analysis of the TLR4, MyD88, TNF-α, and IL-6 mRNA expression levels in rat liver tissues by qRT-PCR. The mRNA expression of (a) TLR4, (b) MyD88, (c) NF-κB, (d) TNF-α, and (e) IL-6 was increased in periodontitis group, in comparison with the control group. Values were shown as mean ± SD. *$p < .05$, **$p < .01$ [Colour figure can be viewed at wileyonlinelibrary.com]

FIGURE 6 Analysis of protein expression levels in rat liver tissues by Western blotting. The results showed that the protein expressions of TLR4, MyD88, NF-κB p65, and p-IκBα were increased in the periodontitis group (A2) versus the control group (A1), while the level of IκBα was declined. Values were shown as mean ± SD. *$p < .05$
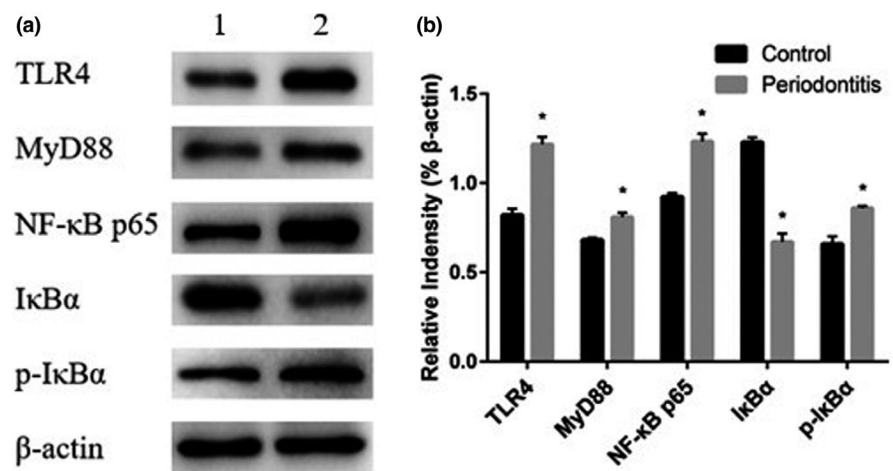
and oxidative stress in serum. Oxidative stress and lipid peroxidation can induce the release of TNF-α and IL-6, which ultimately promote the evolution of hepatic injury. In addition, TNF-α and lipid peroxidation products can increase mitochondrial dysfunction and the production of ROS, which will lead to further increasing the steatosis and starting a vicious circle (Day, 2002; Dockray, 2001; Haque & Sanyal, 2002). Tomofuji et al. (2007) demonstrated that induced periodontitis can cause oxidative damage in liver of rats. Based on these studies, we tested the levels of SOD, T-AOC, and MDA in serum and liver tissues. The data indicated that the levels of SOD and MDA increased and the level of T-AOC decreased in periodontitis group versus the control group.

Many studies have demonstrated that LPS released from periodontal bacteria can transfer to different parts of the body, including liver (Ding, Ren, Yu, Yu, & Zhou, 2018; Fujita et al., 2018;

Hajishengallis, 2015). As discussed before, as pathogen-associated molecular patterns (PAMPs), LPS can activate TLRs, leading to the production of pro-inflammatory cytokines and chemokines. Several studies have shown that high levels of LPS in blood circulation can cause hepatic injury by recruiting some inflammatory cells (Brandl, Kumar, & Eckmann, 2017). Kupffer cells, macrophages derived from liver, play a key role in this pathogenesis. As antigen-presenting cell (APC), they reside in the hepatic sinusoids, are related to host defense, and contribute to endotoxin clearance and inflammatory response. Furthermore, they are able to trigger a cascade of events, resulting in the production of inflammatory cytokines, such as TNF-α and IL-6 (Kudo et al., 2009). MyD88 is the most investigated signaling adaptor for TLRs that mainly is TLR4. The activation of MyD88 results in the upregulation of the NF-κB, ultimately causing the release of inflammatory cytokines. Thus, the mRNA

and protein levels of TLR4, MyD88, NF-κB, TNF-α, and IL-6 were measured by qRT-PCR, Western blot, and histological method. The results showed that the mRNA and protein expression were higher in the periodontitis groups versus the control groups.

However, the present study still has some limitations. In one hand, we only tested the gene and protein levels of TLR4, MyD88, and NF-κB without using specific blockers or activators of signaling pathway. On the other hand, although TNF-α and IL-6 are the most common molecules which are related to inflammation of liver, they cannot represent the whole range of inflammatory cytokines. Therefore, we need to carry out further studies to figure out these points clearly.

5 | CONCLUSION

We have shown that periodontitis induced by ligature can lead to liver inflammation and steatosis of rats. TLR4/MyD88/NF-κB signaling pathway may play a role in this pathogenesis.

AUTHOR CONTRIBUTION
Yiyun Yue: Conceptualization; Data curation; Formal analysis; Investigation; Methodology; Resources; Software; Visualization; Writing-original draft. **Xinchan Liu:** Data curation. **Yan Li:** Data curation. **Boyuan Xia:** Data curation. **Weixian Yu:** Funding acquisition; Project administration; Supervision; Validation.

PEER REVIEW
The peer review history for this article is available at https://publons.com/publon/10.1111/odi.13616.

ORCID
Yiyun Yue 🅧 https://orcid.org/0000-0002-8620-7509
Weixian Yu 🅧 https://orcid.org/0000-0002-3489-7704

REFERENCES
Akinkugbe, A. A., Slade, G. D., Barritt, A. S., Cole, S. R., Offenbacher, S., Petersmann, A., ... Holtfreter, B. (2017). Periodontitis and Non-alcoholic Fatty Liver Disease, a population-based cohort investigation in the Study of Health in Pomerania. *Journal of Clinical Periodontology*, *44*, 1077–1087.

Bellentani, S. (2017). The epidemiology of non-alcoholic fatty liver disease. *Liver International: Official Journal of the International Association for the Study of the Liver*, *37*(Suppl 1), 81–84.

Borrelli, A., Bonelli, P., Tuccillo, F. M., Goldfine, I. D., Evans, J. L., Buonaguro, F. M., & Mancini, A. (2018). Role of gut microbiota and oxidative stress in the progression of non-alcoholic fatty liver disease to hepatocarcinoma: Current and innovative therapeutic approaches. *Redox Biology*, *15*, 467–479.

Brandl, K., Kumar, V., & Eckmann, L. (2017). Gut-liver axis at the frontier of host-microbial interactions. *American Journal of Physiology. Gastrointestinal and Liver Physiology*, *312*, G413–G419.

Brun, P., Castagliuolo, I., Pinzani, M., Palu, G., & Martines, D. (2005). Exposure to bacterial cell wall products triggers an inflammatory phenotype in hepatic stellate cells. *American Journal of Physiology. Gastrointestinal and Liver Physiology*, *289*, G571–G578.

Day, C. P. (2002). Pathogenesis of steatohepatitis. *Best Practice & Research Clinical Gastroenterology*, *16*, 663–678.

Di Paola, R., Marzocco, S., Mazzon, E., Dattola, F., Rotondo, F., Britti, D., ... Cuzzocrea, S. (2004). Effect of aminoguanidine in ligature-induced periodontitis in rats. *Journal of Dental Research*, *83*, 343–348.

Ding, Y., Ren, J., Yu, H., Yu, W., & Zhou, Y. (2018). Porphyromonas gingivalis, a periodontitis causing bacterium, induces memory impairment and age-dependent neuroinflammation in mice. *Immun Ageing*, *15*, 6.

Dockray, G. J. (2001). Transepithelial signaling: Making sense of stomach contents. *Gastroenterology*, *120*, 1279–1281.

Dos Santos, C. J., Cardoso Guimaraes Vasconcelos, A. C., Herlany Pereira Alves, E., Dos Santos, C. A., da Silva, F. R. P., de Carvalho Franca, L. F., ... Vasconcelos D. F. P. (2017). Steatosis caused by experimental periodontitis is reversible after removal of ligature in rats. *Journal of Periodontal Research*, *52*, 883–892.

Eke, P. I., Dye, B. A., Wei, L., Slade, G. D., Thornton-Evans, G. O., Borgnakke, W. S., ... Genco, R. J. (2015). Update on prevalence of periodontitis in adults in the United States: NHANES 2009 to 2012. *Journal of Periodontology*, *86*, 611–622.

Fujita, M., Kuraji, R., Ito, H., Hashimoto, S., Toen, T., Fukada, T., & Numabe, Y. (2018). Histological effects and pharmacokinetics of lipopolysaccharide derived from Porphyromonas gingivalis on rat maxilla and liver concerning with progression into non-alcoholic steatohepatitis. *Journal of Periodontology*, *89*, 1101–1111.

Hajishengallis, G. (2015). Periodontitis: From microbial immune subversion to systemic inflammation. *Nature Reviews Immunology*, *15*, 30–44.

Haque, M., & Sanyal, A. J. (2002). The metabolic abnormalities associated with non-alcoholic fatty liver disease. *Best Practice & Research Clinical Gastroenterology*, *16*, 709–731.

Hegde, R., & Awan, K. H. (2019). Effects of periodontal disease on systemic health. *Disease-a-month*, *65*, 185–192.

Jayakumar, S., & Loomba, R. (2019). Review article: Emerging role of the gut microbiome in the progression of nonalcoholic fatty liver disease and potential therapeutic implications. *Alimentary Pharmacology & Therapeutics*, *50*, 144–158.

Kim, M. H., Seong, J. B., Huh, J. W., Bae, Y. C., Lee, H. S., & Lee, D. S. (2019). Peroxiredoxin 5 ameliorates obesity-induced non-alcoholic fatty liver disease through the regulation of oxidative stress and AMP-activated protein kinase signaling. *Redox Biology*, *28*, 101315.

Kinane, D. F., Stathopoulou, P. G., & Papapanou, P. N. (2017). Periodontal diseases. *Natural Reviews Disease Primers*, *3*, 17038.

Komazaki, R., Katagiri, S., Takahashi, H., Maekawa, S., Shiba, T., Takeuchi, Y., ... Izumi, Y. (2017). Periodontal pathogenic bacteria, Aggregatibacter actinomycetemcomitans affect non-alcoholic fatty liver disease by altering gut microbiota and glucose metabolism. *Scientific Reports*, *7*, 13950.

Konkel, J. E., O'Boyle, C., & Krishnan, S. (2019). Distal Consequences of Oral Inflammation. *Frontiers in Immunology*, *10*, 1403.

Kudo, H., Takahara, T., Yata, Y., Kawai, K., Zhang, W., & Sugiyama, T. (2009). Lipopolysaccharide triggered TNF-alpha-induced hepatocyte apoptosis in a murine non-alcoholic steatohepatitis model. *Journal of Hepatology*, *51*, 168–175.

Lamont, R. J., Koo, H., & Hajishengallis, G. (2018). The oral microbiota: Dynamic communities and host interactions. *Nature Reviews Microbiology*, *16*, 745–759.

Liccardo, D., Cannavo, A., Spagnuolo, G., Ferrara, N., Cittadini, A., Rengo, C., & Rengo, G. (2019). Periodontal Disease: A Risk Factor for Diabetes and Cardiovascular Disease. *International Journal of Molecular Sciences*, 20. https://doi.org/10.3390/ijms20061414

Mester, A., Ciobanu, L., Taulescu, M., Apostu, D., Lucaciu, O., Filip, G. A., … Campian, R. S. (2019). Periodontal disease may induce liver fibrosis in an experimental study on Wistar rats. *Journal of Periodontology*, 90, 911–919.

Moretti, J., & Blander, J. M. (2014). Insights into phagocytosis-coupled activation of pattern recognition receptors and inflammasomes. *Current Opinion in Immunology*, 26, 100–110.

Paik, Y. H., Schwabe, R. F., Bataller, R., Russo, M. P., Jobin, C., & Brenner, D. A. (2003). Toll-like receptor 4 mediates inflammatory signaling by bacterial lipopolysaccharide in human hepatic stellate cells. *Hepatology*, 37, 1043–1055.

Pessoa, L. S., Pereira-da Silva, F. R., Alves, E. H., Franca, L. F., di Lenardo, D., Carvalho, J. S., … Vasconcelos, D. F. (2018). One or two ligatures inducing periodontitis are sufficient to cause fatty liver. *Medicina Oral Patologia Oral Y Cirugia Bucal*, 23, e269–e276.

Potempa, J., Mydel, P., & Koziel, J. (2017). The case for periodontitis in the pathogenesis of rheumatoid arthritis. *Nature Reviews Rheumatology*, 13, 606–620.

Sanyal, A. J., Brunt, E. M., Kleiner, D. E., Kowdley, K. V., Chalasani, N., Lavine, J. E., … McCullough, A. (2011). Endpoints and clinical trial design for nonalcoholic steatohepatitis. *Hepatology*, 54, 344–353.

Sasaki, N., Katagiri, S., Komazaki, R., Watanabe, K., Maekawa, S., Shiba, T., … Izumi, Y. (2018). Endotoxemia by porphyromonas gingivalis injection aggravates non-alcoholic fatty liver disease, disrupts glucose/lipid metabolism, and alters gut microbiota in mice. *Frontiers in Microbiology*, 9, 2470.

Srivastava, M., Neupane, Y. R., Kumar, P., & Kohli, K. (2016). Nanoemulgel (NEG) of Ketoprofen with eugenol as oil phase for the treatment of ligature-induced experimental periodontitis in Wistar rats. *Drug Delivery*, 23, 2228–2234.

Tomofuji, T., Ekuni, D., Sanbe, T., Azuma, T., Tamaki, N., Irie, K., … Takata, T. (2009). Effects of improvement in periodontal inflammation by toothbrushing on serum lipopolysaccharide concentration and liver injury in rats. *Acta Odontologica Scandinavica*, 67, 200–205.

Tomofuji, T., Ekuni, D., Yamanaka, R., Kusano, H., Azuma, T., Sanbe, T., … Takata, T. (2007). Chronic administration of lipopolysaccharide and proteases induces periodontal inflammation and hepatic steatosis in rats. *Journal of Periodontology*, 78, 1999–2006.

Tripathi, A., Debelius, J., Brenner, D. A., Karin, M., Loomba, R., Schnabl, B., & Knight, R. (2018). The gut-liver axis and the intersection with the microbiome. *Nature Reviews Gastroenterology & Hepatology*, 15, 397–411.

Van De Wier, B., Koek, G. H., Bast, A., & Haenen, G. R. (2017). The potential of flavonoids in the treatment of non-alcoholic fatty liver disease. *Critical Reviews in Food Science and Nutrition*, 57, 834–855.

Vasconcelos, A., Vasconcelos, D. F. P., Pereira da Silva, F. R., de Carvalho Franca, L. F., Alves, E. H. P., Lenardo, D. D., … de Oliveira, A. P. (2019). Periodontitis causes abnormalities in the liver of rats. *Journal of Periodontology*, 90, 295–305.

Vasconcelos, D. F., Pereira da Silva, F. R., Pinto, M. E., Santana, L. A., Souza, I. G., Miranda de Souza, L. K., … Soares de Oliveira, J. (2017). Decrease of Pericytes is Associated With Liver Disease Caused by Ligature-Induced Periodontitis in Rats. *Journal of Periodontology*, 88, e49–e57.

Wang, R. P., Ho, Y. S., Leung, W. K., Goto, T., & Chang, R. C. (2019). Systemic inflammation linking chronic periodontitis to cognitive decline. *Brain, Behavior, and Immunity*. https://doi.org/10.1016/j.bbi.2019.07.002

Xu, Y., & Wei, W. (2006). A comparative study of systemic subantimicrobial and topical treatment of minocycline in experimental periodontitis of rats. *Archives of Oral Biology*, 51(9), 794–803. https://doi.org/10.1016/j.archoralbio.2006.03.018

Xue, L., Su, L., Zhao, L., Li, J., Du, Y., & Yu, X. (2018). Cyclophilin a increases CD68(+) cell infiltration in rat experimental periodontitis. *Journal of Molecular Histology*, 49, 157–164.

Yoneda, M., Naka, S., Nakano, K., Wada, K., Endo, H., Mawatari, H., … Nakajima, A. (2012). Involvement of a periodontal pathogen, Porphyromonas gingivalis on the pathogenesis of non-alcoholic fatty liver disease. *BMC Gastroenterology*, 12, 16.

Younossi, Z., Anstee, Q. M., Marietti, M., Hardy, T., Henry, L., Eslam, M., … Bugianesi, E. (2018). Global burden of NAFLD and NASH: Trends, predictions, risk factors and prevention. *Nature Reviews Gastroenterology & Hepatology*, 15, 11–20.

Yu, X., Gong, Z., Lin, Q., Wang, W., Liu, S., & Li, S. (2017). Denervation effectively aggravates rat experimental periodontitis. *Journal of Periodontal Research*, 52, 1011–1020.

Yu, X., Liu, H., Liu, S., Chen, X., Zhao, X., Du, Y., & Li, S. (2019). Periodontal ligament-associated protein-1 gets involved in experimental periodontitis. *Journal of Periodontal Research*, 54, 180–189.